On the Validity of the No-Slip Condition in Nanofluidics

P. Koumoutsakos[1,2], R. L. Jaffe[3], T. Werder[1,4] and J. H. Walther[1,5]
[1]Institute of Computational Science, Swiss Federal Institute of Technology
CH-8092 Zürich, Switzerland
[2]petros@inf.ethz.ch
[3]NASA Ames Research Center, USA. rjaffe@mail.arc.nasa.gov
[4]werder@inf.ethz.ch, [5]walther@inf.ethz.ch

ABSTRACT

We study the applicability of the no-slip boundary conditions in nanoscale geometries. We conduct NEMD simulations for a prototypical system of water graphite surface. For the planar Couette flow, we find a slip length of 64 nm at physiological conditions (1 atm and 300 K), that decreases with increasing system pressure to a value of 31 nm at 1000 bar. Changing the properties of the interface from hydrophobic to strongly hydrophilic reduces the slip length to 14 nm. We furthermore study the flow of water past an array of carbon nanotubes mounted in an inline arrangement with a spacing of 16.4×16.4 nm. For tube diameters of 1.25 and 2.50 nm we find drag coefficients in good agreement with the macroscopic, Stokes-Oseen solution. For this flow past the carbon nanotubes, we find the no-slip condition is valid to within the definition of the position of the interface.

Keywords: no-slip condition, hydrophobic, Couette flow, carbon nanotubes, nanofluidics, drag forces

1 INTRODUCTION

Macroscopic, Navier-Stokes modeling of problems in nano-fluidics may prove to be a computationally cost effective alternative to molecular dynamics simulations usually employed at these length scales [1], provided a suitable macro-scopic model can be found for the complex interactions governing the fluid-solid interface. At hydrophobic surfaces these interactions result in strong density fluctuations, anisotropic orientation of the water molecules [2], and for high density solids, a finite fluid velocity (ΔU) at the interface [3, 4, 5]. Thus while the kinematic boundary condition of impermeability follows naturally from the definition of a fluid-solid interface, the issues relating to the momentum transfer at the interface and governing the dynamics of the problem is less clear. At moderate shear rates the fluid may be considered Newtonian [6], and the slip velocity may be described by the linear relation:

$$\Delta U = L_s \frac{\partial u}{\partial y}, \qquad (1)$$

where L_s is the slip length and $\partial u/\partial y$ the shear rate at the surface. Experimental evidence of slip has been demonstrated in studies of water in hydrophobized quartz capillaries [4] and in drainage experiments [5] with slip lengths of 30 ± 10 nm and 38 ± 2 nm, respectively. While most experiments have focused on the presence of slip at hydrophobic surfaces and on the possible validity of the no-slip condition at hydrophilic surfaces, recent colloid probe experiments of water on mica and glass have indicated a persistent slip of 8–9 nm at these hydrophilic surfaces [7]. Molecular dynamics simulations of Poiseuille flow [8, 9] and planar Couette flow [10, 11] of simple Lennard-Jones fluids confined between Lennard-Jones solids have demonstrated the presence of both slip, no-slip and locking (negative slip length) depending on the "corrugation" of the surface. Thus, no-slip and locking are observed for low density solids, and slip is found to occur at strongly non-wetting interfaces, or for high density solids. In a recent study of methane confined between dense, graphite surfaces Sokhan *et al.* [12] found the slip to be fairly insensitive to the wetting properties of the surface, but to depend strongly on the density of the solid.

2 NON-EQUILIBRIUM MOLECULAR DYNAMICS

The present study employs non-equilibrium molecular dynamics (NEMD) simulations of water at hydrophobic, dense (graphite) surfaces. First we consider water in a planar Couette flow, to study the influence of the system pressure and of wetting behaviour of the interface on the slip length. The second part involves water flowing past an array of carbon nanotubes to study the effect of curvature on the slip length. In both studies the graphite and the carbon nanotubes are treated as rigid structures.

The carbon-water interaction energy is modeled by a Lennard-Jones potential between the carbon and oxygen atoms, $U(r_i) = 4\epsilon_{CO} \sum_i (\sigma_{CO}/r_i)^{-12} - (\sigma_{CO}/r_i)^{-6}$, where the index i runs over all pairs of C and O atoms and r_i is the distance between the atoms in the i-th pair. The parameters of the potential are obtained from molecular dynamics simulations of the contact angle of water droplets on graphite [14]. All non-bonded interaction are truncated at 1 nm using a smooth tapering of the potential [15].

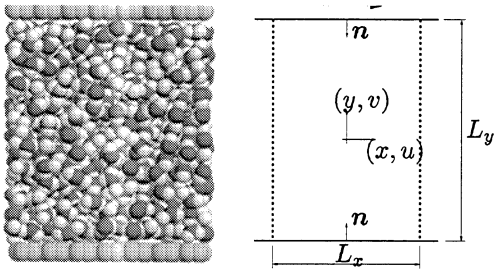

Figure 1: Sketch of the planar Couette flow problem. L_x and L_y denote the length of the unit cell in the streamwize (x) and wall normal direction (y). The upper wall is forced to move with a constant velocity (U) and periodic boundary conditions are enforced in the streamwize and the spanwize (z) directions.

3 RESULTS AND DISCUSSION

The results from the Couette and carbon nanotube studies are presented in terms of the time average profiles of the density and streaming velocity

$$\boldsymbol{v}_k = \frac{\sum_i^{n_k} m_i \boldsymbol{u}_i}{\sum_i^{n_k} m_i}, \qquad (2)$$

where m_i and $\boldsymbol{u}_i$ denote the mass and velocity of the i-th atom, and n_k denotes the number of atoms in the k-th bin of volume V_k. The statistics are collected in Cartesian and polar bins for the two Couette and flow past the carbon nanotubes, respectively.

3.1 Couette flow

The simulations of the Couette flow involve 1040 water molecules confined between single graphite sheets with a spacing of approximately 4.6 nm depending on the system pressure. The size of the system in the streamwize (L_x) and spanwize (L_z) direction is 2.98×2.46 nm (Figure 1). The water molecules are initially placed on a regular lattice and the system is equilibrated for 40 ps to obtain a system temperature of 300 K and the desired pressure. Periodic boundary conditions are imposed in the streamwize and spanwize directions, and free space conditions are assumed in the wall normal (y) direction. A Berendsen thermostat is applied to adjust both the temperature and pressure. The pressure is measured from the total normal forces acting on the graphite sheets. The upper graphite wall is set into motion after 50 ps with a constant velocity (U) of 100 ms^{-1} throughout the 6 ns of simulation. The system did not experience any appreciable viscous heating during the course of the simulation. The results are summarized in Table 1.

We first consider the influence of the system pressure on the amount of slip for system pressures of 10, 200, 500, and 1000 bar using the reference carbon-water interaction potential. At these pressures the time average profiles of the streaming velocity shown in Figure 2 reveal a decreasing slip length for increasing pressure, resulting in a slip of 63, 63, 42, and 31 nm, respectively. The peaks in the profiles for $|x| > 2$ nm are caused by the poor sampling at the interfaces. The large fluctuations in the pressure typically for these small systems result in similar results for the 10 and 200 bar system. The tendency of decreasing slip for increasing system pressures is in agreement with the recent NEMD simulations of Lennard-Jones fluids confined between Lennard-Jones solids by Barrat and Bocquet [8]. Moreover, the magnitude of the slip is in good agreement with the experimental values of 30–40 nm cf. [4, 5].

Next we consider the influence of the wetting properties of the graphite-water interface by varying the strength of the Lennard-Jones interaction potential through an increase of the ϵ_{CO} parameter from the reference value of 0.4389 kJ mol^{-1} by 50 % and 100 % corresponding to 0.6594 kJ mol^{-1} and 0.8778 kJ mol^{-1}, respectively. The

Case	ϵ_{CO} (kJ mol^{-1})	P (bar)	L_y (nm)	L_s (nm)
1	ref.	10	4.72	63
2	ref.	200	4.71	63
3	ref.	500	4.60	42
4	ref.	1000	4.50	31
5	+50 %	200	4.66	33
6	+100 %	200	4.59	14

Table 1: Simulation cases for the planar Couette flow conducted at 300 K and pressures (P) of 10, 200, 500, and 1000 bar, respectively. The reference water-graphite van der Waals interaction given by ϵ_{CO} is 0.4389 kJ mol^{-1} [14]. L_y denotes the spacing between the graphite surfaces, and L_s the slip length.

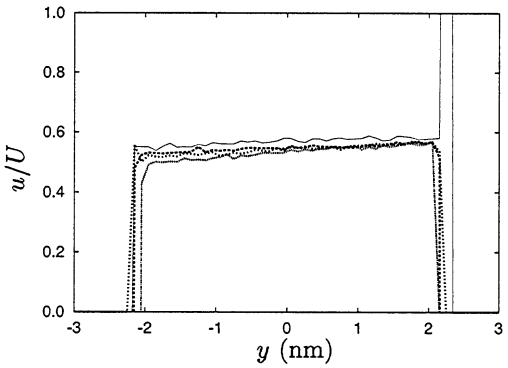

Figure 2: Time average streaming velocity profiles in a Couette flow as function of the system pressure: — : 10 bar (case 1); – – : 200 bar (case 2); - - : 500 bar (case 4); ··· : 1000 bar (case 4).

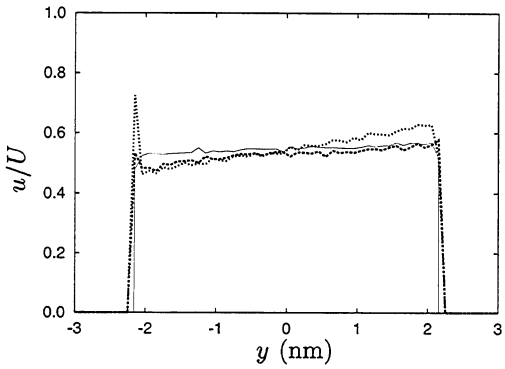

Figure 3: Time average streaming velocity profiles in a Couette flow as function of the wetting properties of the fluid-solid interface: —: $\epsilon_{CO} = 0.4389\,\mathrm{kJ\,mol^{-1}}$ (case 2); – –: $\epsilon_{CO} = 0.6594\,\mathrm{kJ\,mol^{-1}}$ (case 5); - - : $\epsilon_{CO} = 0.8778\,\mathrm{kJ\,mol^{-1}}$ (case 6).

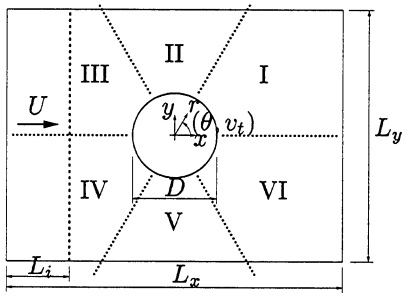

Figure 4: Sketch of the carbon nanotube-water system. D denotes the diameter of the carbon nanotube, L_x the size of the system in the streamwise direction, and L_y and L_z the height and width, respectively. The velocity of the center of mass of the water molecules contained in the "inlet" region (L_i) of the computational box is fixed to the desired value (U).

macroscopic contact angle for these interaction potentials for water droplets on graphite is 85°, 30°, and 0°, respectively [14]. The time average streaming velocity shown in Figure 3 reveals a marked influence on the slip length. Thus, the slip decreases from 63 nm for the reference interaction potential to 33 and 12 nm for the 50 % and 100 % systems, the latter in good agreement with the experimental value of 8–9 nm for water at a hydrophilic surface [7].

3.2 Flow past an array of carbon nanotubes

The flow past an array of carbon nanotubes is considered for tube diameters of 1.25 nm and 2.50 nm to study the effect of curvature on the no-slip boundary condition and to compare the fluid forces acting on the array with macroscale Navier-Stokes models. The carbon nanotubes are (16,0) and (32,0) zigzag tubes, located at the center of the computational box with dimensions of $16.4 \times 16.4 \times 2.1$ nm. The total number of water molecules is approximately 18500, and the carbon nanotubes consist of 320 and 640 atoms for the 1.25 nm and 2.50 nm tubes, respectively.

The onset flow speed ($U = 50\,\mathrm{ms^{-1}}$) is chosen sufficiently above the thermal noise to allow efficient sampling, and yet corresponding to a low Mach number (Ma < 0.05) to avoid compressibility effects. During the first 4 ps of the 8 ps equilibration, the volume of the computational box is adjusted to match the target density of water (here $\rho = 0.997\,\mathrm{g\,cm^{-3}}$) in the far-field, i.e. in the region defined by $r > R + \delta$, where $R = D/2$ is the tube radius, and $\delta = 0.8$ nm is chosen to exclude the region containing the density variations in the vicinity of the carbon nanotube [15]. The flow is initially quiescent and impulsively turned on after 6 ps while maintaining the thermostat for the remaining 2 ps of the equilibration. The spatially averaged streaming velocity is computed during the simulation and subtracted to allow equilibration of the peculiar velocities only. 0.76 ns simulation was less than 8 K. A body force is imposed in a 3 nm (L_i) wide inlet to ensure the prescribed flow speed (U) cf. Figure 4. The time average density and streaming velocity profiles are sampled along the 6 radial bins as shown in Figure 4. Both profiles exhibit symmetry across the x-axis, whereas asymmetries are discernible in the density profiles in the streamwise direction, in the vicinity of the carbon nanotube cf. Figure 5. The location of the density extrema are similar for the three profiles, with the first peak located at $r - R = 0.32$ nm coinciding with the van der Waals equilibrium distance (σ_{CO}). However, the peak values decrease from $3.0\,\mathrm{g\,cm^{-3}}$ at the upstream direction (section III) to $2.8\,\mathrm{g\,cm^{-3}}$ and $2.6\,\mathrm{g\,cm^{-3}}$ for the sections II and I, respectively. Since the far-field density is constant with a value of approximately $1.0\,\mathrm{g\,cm^{-3}}$, the observed asymmetry is ascribed to a local compression of the water near the surface. The amount of slip experienced for these systems is extracted from the tangential component (v_t) of the streaming velocity for the sections II and V shown in Figure 6. The velocity profiles are similar for the two cases but reach different free-stream values due to the different blockage ($(D - L_y)/L_y$) experienced by the flow. Since the macro-scale Reynolds number (Re) based on the tube diameter and the fluid viscosity (ν) is less than unity, the velocity profile is fitted to the Stokes velocity field for a single circular cylinder [16]

$$v_t = a \log\left(\frac{r}{R}\right) + b + c\frac{R^2}{r^2}, \qquad (3)$$

where a, b, and c, are parameters of the fit. The fit is performed for the data shown in Figure 6 in the interval

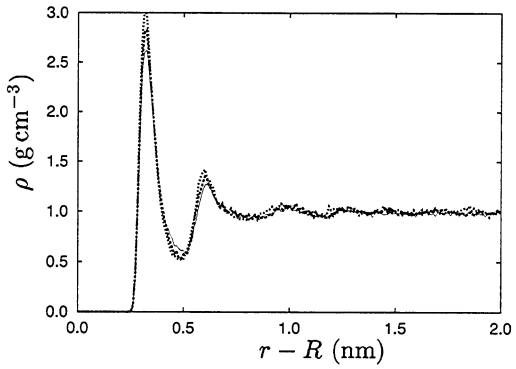

Figure 5: The time average radial density profile for the flow past an array of 2.50 nm carbon nanotube. The profiles are sampled upstream, at the mid-section and downstream sections: —: section I; – –: section II; - - : section III.

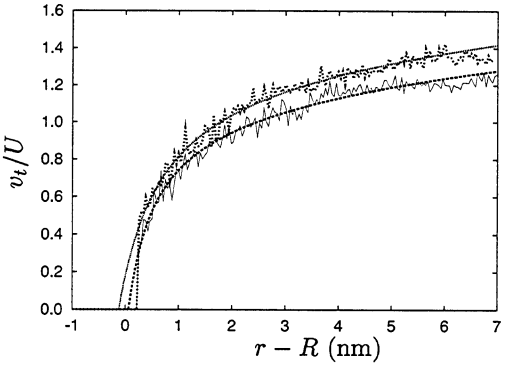

Figure 6: The time average tangential component of the streaming velocity for the flow past an array of carbon nanotubes. The profiles are sampled from section II and V and compared with equation (3) the for the 1.25 nm tube: —: measured; – –: fit and the 2.50 nm tube: - - : measured; $\cdots$: fit.

$r \in [R + \sigma_{CO} : 7\,\text{nm}]$. We find within the uncertainty of the fit, and to within the accuracy of the definition of the location of the surface, the no-slip condition is satisfied, i.e., $L_s < \sigma_{CO}$.

Finally, we consider the fluid forces acting on the carbon nanotube array. The streamwize component of the force (f_x) is compared with the Stokes-Oseen drag for the flow past an array of two-dimensional circular cylinders [17]. For the two cases, the Stokes-Oseen drag coefficients are 112 and 81 for the 1.25 nm and 2.50 nm carbon nanotubes, respectively. The measured forces are sampled from 0.40 ns to 0.66 ns using 13 samples of 20 ps each. The corresponding drag coefficients are 134 ± 20 and 85 ± 20, both in excellent agreement with the Stokes-Oseen values.

ACKNOWLEDGEMENTS

Support from the CTR Summer Program 2002 Stanford University is greatly appreciated.

REFERENCES

[1] J. Koplik and J. R. Banavar, Annu. Rev. Fluid Mech. ***27****, 257 (1995).*

[2] C. Y. Lee, J. A. McCammon, and P. J. Rossky, J. Chem. Phys. ***80****, 4448 (1984).*

[3] H. Helmholtz and G. von Piotrowski, Sitzungsberichte der Kaiserlich Akademie der Wissenschaften ***40****, 607 (1860).*

[4] N. V. Churaev, V. D. Sobolev, and A. N. Somov, J. Coll. Interface Sci. ***97****, 574 (1984).*

[5] J. Baudry, E. Charlaix, A. Tonck, and D. Mazuyer, Langmuir ***17****, 5232 (2001).*

[6] W. Loose and S. Hess, Rheol. Acta ***28****, 91 (1989).*

[7] E. Bonaccurso, M. Kappl, and H.-J. Butt, Phys. Rev. Lett. ***88****, 076103 (2002).*

[8] J.-L. Barrat and L. Bocquet, Phys. Rev. Lett. ***82****, 4671 (1999).*

[9] K. P. Travis and K. E. Gubbins, J. Chem. Phys. ***112****, 1984 (2000).*

[10] P. A. Thompson and S. M. Troian, Nature ***389****, 360 (1997).*

[11] M. Cieplak, J. Koplik, and J. R. Banavar, Phys. Rev. Lett. ***86****, 803 (2001).*

[12] V. P. Sokhan, D. Nicholson, and N. Quirke, J. Chem. Phys. ***115****, 3878 (2001).*

[14] T. Werder, J. H. Walther, R. L. Jaffe, T. Halicioglu, and P. Koumoutsakos, J. Phys. Chem. B p. accepted (2003).

[15] J. H. Walther, R. Jaffe, T. Halicioglu, and P. Koumoutsakos, J. Phys. Chem. B ***105****, 9980 (2001).*

[16] G. K. Batchelor, An Introduction To Fluid Dynamics *(Cambridge University Press, 1967), 1st ed.*

[17] R. F. Probstein, Physicochemical Hydrodynamics *(Butterworts Publishers, 1989).*